JPET Fast Forward. Published on September 20, 2005 as DOI: 10.1124/jpet.105.092106

Multiple Cellular Electrophysiological Effects of a Novel Antiarrhythmic Furoquinoline Derivative HA-7, in Guinea Pig Cardiac Preparations

Gwo-Jyh Chang, Ming-Jai Su, Sheng-Chu Kuo, Tsung-Ping Lin, and Ying-Shiung Lee

Graduate Institute of Clinical Medicinal Sciences, College of Medicine, Chang Gung University, Tao-Yuan, Taiwan (G.-J.C., Y.-S.L.); Pharmacological Institute, College of Medicine, National Taiwan University, Taipei, Taiwan (M.-J.S.); Institute of Phamaceutical Chemistry, China Medical University, Taichung, Taiwan (S.-C.K., T.-P.L.); The First Cardiovascular Division of Medicine, Chang Gung Memorial Hospital, Taipei, Taiwan (Y.-S.L.)

Running title: Multiple cardiac electrophysiological effects of HA-7

Author for correspondence: **Gwo-Jyh Chang**

Graduate Institute of Clinical Medicinal Sciences,

College of Medicine,

Chang Gung University,

5 Fu-Shing St, Kwei-Shan,

Tao-Yuan, Taiwan

Tel: 886-3-328-1200 Ext. 8872

Fax: 886-3-328-0170

E mail: gjchang@adm.cgmh.org.tw

The number of text pages: 23

The number of tables: 3

The number of figures: 9

The number of references: 36

The number of words in the *Abstract*: 248

The number of words in the *Introduction*: 492

The number of words in the *Discussion*: 1500

Abbreviations: AERP, atrial effective refractory period; AF, atrial fibrillation; AH, atrio-His bundle conduction interval; APA, action potential amplitude; $APD_{25, 50, 90}$, action potential duration measured at 25, 50 and 90% repolarization; AVNERP, AV nodal effective refractory period; BCL, basic cycle length; DMSO, dimethylsulfoxide; EAD, early afterdepolarization; E-4031, *N*-(4-

JPET Fast Forward. Published on September 20, 2005 as DOI: 10.1124/jpet.105.092106
This article has not been copyedited and formatted. The final version may differ from this version.

[(1-[2-(6-methyl-2-pyridyl)ethyl]-4-piperidyl)-carbonyl]phenyl)methanesulfonamide; HA-7, *N*-benzyl-7-methoxy-2,3,4,9-tetrahydrofuro[2,3-*b*]quinoline-3,4-dione); HPFRP, His-Purkinje system functional refractory period; HV, His-ventricular conduction interval; IC_{50}, concentration that produces 50% of maximal inhibition; I_{Ca}: Ca^{2+} inward current; $I_{K(Ado)}$: adenosine-activated K^+ current; I_{K1}: inward rectifier K^+ current; I_{Kr}: fast component of the delayed rectifier K^+ current; I_{Ks}: slow component of the delayed rectifier K^+ current; I_{Na}: Na^+ inward current; I_{to}: transient outward K^+ current; I_{SS}: steady-state outward K^+ current; RMP, resting membrane potential; SA, sinoatrial conduction interval; VERP, ventricular effective refractory period; VF, ventricular fibrillation; V_{max}, maximal upstroke velocity of action potential; VRT, ventricular repolarization time; VT, ventricular tachycardia; WCL, Wenckebach cycle length.

Recommended section: Cardiovascular

Abstract

We studied the electrophysiological and antiarrhythmic actions of HA-7, a furoquinoline alkaloid derivative, in guinea pig heart preparations. In the perfused whole heart model, HA-7 caused a prolongation in the basic cycle length, ventricular repolarization time and the AV nodal Wenckebach cycle length and prolonged the refractory period of the atrium, AV node and His-Purkinje system. The atrioventricular conduction interval was also prolonged in a frequency-dependent manner. In isolated hearts, HA-7 significantly raised the threshold for experimental atrial fibrillation and reduced the occurrence of reperfusion-induced ventricular fibrillation. Conventional microelectrode recording study shows that HA-7, but not d-sotalol, prolonged the action potential duration (APD) and decreased the maximum rate of depolarization in isolated atrial strips. In ventricular papillary muscles, higher concentrations of HA-7 caused a prolongation of APD_{90} in a frequency-independent manner while d-sotalol exerted a reverse frequency-dependent action on this parameter. Whole-cell patch clamp results on ventricular myocytes indicate that HA-7 decreased both the slow (I_{Ks}) (IC_{50}=4.8 μM) and fast component (I_{Kr}) (IC_{50}=1.1 μM) of the delayed rectifier K^+ currents. Similar results could also be observed in atrial myocytes. The inward rectifier K^+ current (I_{K1}) was also reduced somewhat by HA-7. HA-7 also suppressed the Na^+ inward current (I_{Na}) (IC_{50}=2.9 μM) and inhibited the L-type Ca^{2+} current (I_{Ca}) (IC_{50}=4.0 μM, maximal inhibition=69%) to a lesser extent. We conclude that HA-7 blocks multiple ionic currents and that these affect the electrophysiological properties of the conduction system as well as the myocardial tissues and may contribute to its antiarrhythmic efficacy.

Introduction

Atrial and ventricular tachyarrhythmias are believed to play a major role in human morbidity and mortality. Unfortunately, most currently available antiarrhythmic agents are less than ideal in this therapeutic setting. Since the negative outcome of the Cardiac Arrhythmia Suppression Trial (Echt et al., 1991), class III antiarrhythmics attracted attention and were expected to be more beneficial than class I agents for treatment of life-threatening ventricular tachyrhythmias and suppressing sudden cardiac death in patients with such risks (Singh and Nademanee, 1985). In recent years, selective blockers of the cardiac delayed rectifier K^+ current (I_K), especially the rapid component (I_{Kr}), have been developed (for a review, see Tamargo et al., 2004). Although these agents are effective in the termination and prevention of experimentally induced arrhythmias, the therapeutic potential of these drugs in severely sick patients is questionable (Waldo et al., 1996). Consequently, the search for new types of antiarrhythmic drug to treat malignant cardiac arrhythmias remains an important area of research (Sanguinetti and Bennett, 2003). Recently, much attention has been focused on the antiarrhythmic drugs with multiple modes of action, i.e., acting on different ion channels and/or receptors, with the expectation that such agents may be more effective for therapy and devoid of serious cardiac side effects (Mátyus et al., 1997; Amos et al., 2001).

HA-7 is a novel tetrahydro-furoquinoline alkaloid derivative that has been synthesized recently. We previously demonstrated that HA-7 could reverse the cardiac arrhythmias induced by postischemic reperfusion in isolated rat hearts and produce a moderate positive inotropic effect in rat cardiac tissues (Su et al., 1997). In the same study, it was shown that this antiarrhythmic activity may be related to the predominant blockade of the I_{to}, a major repolarizing current in rat heart (Josephson et al., 1984), I_{SS} and Na^+ channels. Thus, HA-7

may exert mixed class I and stronger class III antiarrhythmic properties (Su et al., 1997). In fact, most of the class III antiarrhythmic agents such as sotalol, dofetilide or amiodarone are known to prolong cardiac APD and suppress re-entrant arrhythmia primarily via the blockade of the I_K which is absent in rat cardiomyocytes but exists prominently as the main repolarizing current in guinea pig (Hume and Uehara, 1985) and human myocardium (Li et al., 1996). Therefore, the present study was conducted to examine whether HA-7 could also exert antiarrhythmic, electromechanical, and ion channel modifying actions in guinea pig heart preparations and to compare its effects with those of a typical class III agent d-sotalol (Hohnloser and Woosley, 1994). In this study, the antiarrhythmic effect of HA-7 was evaluated on both the electrical stimulation-induced atrial fibrillation and the reperfusion-induced ventricular tachyarrhythmias in Langendorff-perfused guinea pig hearts. The electrophysiological activity of HA-7 on the conduction system was assessed in perfused isolated hearts, while the mechanical and electrophysiological effects of HA-7 were assessed in guinea pig atrial strips and ventricular papillary muscles. Further investigations on ionic currents were also performed using the patch-clamp technique in guinea pig isolated cardiomyocytes.

Materials and Methods

All experiments were performed in accordance with the internationally accepted guidelines. Studies were approved by the Institute Committee of the Animal Care of the University of Chang Gung College of Medicine. Guinea pigs were housed in the animal care facility at the Chang Gung Memorial Hospital (Tao-Yuan, Taiwan). All animals were housed with a 12 h light/dark cycle. Food (standard rat chow) and water were available *ad libitum*.

Intracardiac electrocardiogram recording experiment

Animal preparation. Adult male Hartly guinea pigs (250-300 g body weight, purchased from the Laboratory Animal Center of National Taiwan University Hospital) were anesthesized with sodium pentobarbital (50 mg/kg, i.p.) and given heparin (300 units/kg, i.p.). Following anesthesia, the heart was excised via thoracotomy and the ascending aorta was retrogradely perfused at a rate of 4 ml/min/g cardiac tissue with normal Tyrode solution (Chang et al., 2002). The solution was continuously gassed with 95% O_2 and 5% CO_2 to give a pH of 7.4 and was maintained at 37°C. To pace the atria, a high right atrial electrode was placed near the junction of the superior vena cava and right atrium. A bipolar electrode consisting of a tungsten spring-soldered silver wire was placed on the endocardium near the apex of the triangle of Koch to record the His bundle electrograms. In the next stage, the tips of the ventricular recording electrode were placed on opposite sides of the epicardium near the ventricular apex, thereby providing a recognizable T wave. In addition, a ventricular pacing electrode was placed on the pericardium near the right ventricular apex. Pacing studies were performed by utilizing a programmable stimulator (DTU 215, Bloom Electrophysiology, Fischer Imaging Co., CO, U.S.A.). A pacing stimulus of 1 ms in duration and twice the diastolic threshold voltage was applied to the preparation through the bipolar atrial or

ventricular electrodes. The electrograms were continuously monitored on an oscilloscope (TDS520D, Tektronix, Inc., OR, U.S.A.) and pertinent data were recorded on a chart recorder (WindowGraf, Gould Instrument Systems, Inc., OH, U.S.A.).

Experimental protocol. An average of 4 stable cycle lengths of spontaneous heartbeats was taken as the basic cycle length. The right atrium was then paced at a constant rate that was slightly faster than the spontaneous heart rate. At this constant pacing rate, the intra-atrial (SA), AV nodal (AH) and His-Purkinje (HV) regions as well as the ventricular repolarization time (VRT) were measured. Incremental right atrial pacing was used to determine the Wenckebach cycle length, at which the 1:1 AV nodal conduction pattern was lost. Atrial premature extra-stimulation (S_2) was then delivered to the high right atrium after a train of constant rate atrial pacing (S_1S_1) for 8 beats to obtain the refractory periods of the atria, AV node, and His-Purkinje system. Ventricular effective refractory period was similarly determined using a ventricular extrastimulation study protocol.

Evaluation of antiarrhythmic properties

Global ischaemia/reperfusion-induced arrhythmias. The isolated guinea pig heart was retrogradely perfused through the aorta with normal Tyrode solution at a constant perfusion pressure. A PE60 cannula attached to a side-arm of the constant-pressure Langendorff perfusion apparatus was placed in the right atrium. Following a 10-min equilibration period, hearts were administered drug or vehicle for 10 min. After this pre-ischaemic period, the aortic cannula was clamped to terminate aortic flow and to institute global no-flow ischaemia. Simultaneously with ischemia onset, the right atrial cannula was opened to enable intracavitary superfusion. The rate of atrial superfusion flow was controlled at 6 ml/min to maintain a HR of ~ 200 beats/min. The electrograms were recorded from a low

atrial and a ventricular recording electrode and were continuously monitored on an oscilloscope and pertinent data were recorded on a chart recorder. After 30-min, the aortic cannula was unclamped to permit reperfusion while the right atrial superfusion cannula was clamped and the duration and incidence of arrhythmias was recorded. Vehicle or drug was included in the perfusion solution throughout the time after the pre-ischaemic period.

Measurement of atrial fibrillation threshold (AFT). Previous studies have shown that atrial vulnerability is enhanced by adenosine, which causes shortening of APD and refractoriness (Kabell et al., 1994; for a review, see van der Hooft et al., 2004). We induced AF with a combination of adenosine and electrical stimulation in Langendorff-perfused guinea pig hearts. The fibrillating current was generated from a programmable stimulator (DTU 215) and consisted of a train of 50 square wave pulses of 2-ms duration at a frequency of 50 Hz for 1 s. The pulse train was delivered to the right atrium after every eighth basic paced beat. The current was increased gradually from an intensity twice the diastolic threshold. AFT was defined as the minimum amount of current required to induce AF which was sustained for at least 30 s. To avoid damaging the atrial tissue, we did not deliver a current greater than 14 mA. If AF could not be induced when the current was increased to 14 mA, the AFT was provisionally determined to be 14.1 mA.

Electromechanical recordings

Action potentials were recorded from guinea pig cardiac muscle preparations with a conventional intracellular recording technique (Chang et al., 2002). Briefly, the left atrial strip or ventricular papillary muscle was placed in a tissue chamber and perfused at a rate of 20 ml/min with normal Tyrode solution. The perfusing solution was oxygenated (95% O_2 and 5% CO_2) and kept at 37°C with a temperature controller. External stimuli (1 ms duration, 1.5

times the diastolic threshold voltage) were delivered at a basic rate of 1 Hz by an electronic stimulator (S88, Grass, W. Warwick, RI, U.S.A.) via bipolar platinum electrodes. Each preparation was stretched to a length at which maximum developed force was evoked and allowed to equilibrate for at least 1.5 to 2 hrs before the commencement of the experiments. Transmembrane potentials were amplified with Axoclamp 2B amplifier (Axon Instruments Inc., Foster City, CA, U.S.A.) and the mechanical response was measured with a bridge amplifier (Quad Bridge Amp, ADInstruments, NSW, Australia). Action potentials and contractions were recorded by a digital recorder (PowerLab/4sp, ADInstruments) via Chart software (Version 4.0.2, ADInstruments) for off-line analysis.

Single cell isolation

Single atrial and ventricular cells from adult guinea pigs were enzymatically dissociated as described previously (Isenberg and Klöckner, 1982). In brief, the excised heart was mounted on a modified Langendorff perfusion system and retrogradely perfused through the aorta with a normal HEPES-buffered Tyrode's solution (pH 7.4) gassed with 100% O_2 and maintained at 37±0.2°C. The perfusion medium was then changed to a nominally Ca^{2+}-free HEPES-buffered Tyrode's solution. After 5 min, the perfusate was switched to the same solution containing 0.3 mg/ml collagenase (Type II, Sigma-Aldrich Chem. Co., St. Louis, MO, U.S.A.) and 0.1 mg/ml protease (Type XIV, Sigma-Aldrich). After 7-15 min digestion, the residual enzyme solution was removed by more than 5 min perfusion with "modified KB medium" (Isenberg and Klöckner, 1982). Thereafter, the atrium was separated from the ventricle, and myocytes from both tissues were dispersed and then stored in KB medium for later use. Only quiescent and Ca^{2+}-tolerant cells with clear striations were used for experiments.

Voltage clamp recording

Whole-cell recordings were performed following the technique described by Hamill et al. (1981). Atrial or ventricular cells were bathed at room temperature (25-27°C) in a normal Tyrode's solution. Patch electrodes were fabricated from glass capillaries (o.d.: 1.5 mm, i.d. 1.0 mm; A-M Systems, Carlsborg, WA, U.S.A.) using a two-stage vertical puller (model PP-830, Narishige, Tokyo, Japan) and a microforge (model MF-830, Narishige). The electrode was 2-5 MΩ when filled with the pipette solution. Membrane currents were recorded using an integrating patch clamp amplifier (Axopatch 200B, Axon). Command pulses were generated by a 16-bit D/A converter (digidata 1320A, Axon) controlled by the pCLAMP software (8.0.2, Axon). Electrode junction potentials (5-10 mV) were measured and compensated before formation of the pipette-membrane seal. A high resistance seal (5-10 GΩ) was obtained before the disruption of the membrane patch. Usually, more than 5 min was allowed for adequate cell dialysis after disruption of the membrane patch.

During measurement of K^+ currents, I_{Ca} were blocked by addition of 5 μM nifedipine to the bathing solution, and Na^+ and T-type Ca^{2+} channels were voltage-inactivated by maintaining the holding potential at -40 mV. To study the effect of HA-7 on I_{Ks}, 5 μM E4031 (Sanguinetti and Jurkiewicz, 1990) was used to block I_{Kr}. When the effect on I_{Kr} was measured, 30 μM chromanol 293B (Bosch et al., 1998) was used to block I_{Ks}. For measurement of Ca^{2+} and Na^+ inward currents, the K^+ currents were blocked by adding CsCl (2 mM) to the bathing solution and internal dialysis of the cells with Cs^+ and TEA-containing pipette solution. I_{Na} was studied in a nifedipine (5 μM)-containing low Na^+ Tyrode solution ($[Na^+]$ = 54 mM, with NaCl replaced by N-methyl-D-glucamine) and dialysis of the cell with Na^+ containing (10 mM) Cs^+ pipette solution.

Time-dependent I_K amplitude was measured as the difference from the initial

instantaneous current, after settling of the capacity transient, to the final current level during a given voltage step to various test potentials. I_K tail current amplitude was measured as the difference from the steady-state holding current level to the peak tail current amplitude. Inward rectifier K^+ current (I_{K1}) was measured as the difference from the zero current level at the end of 200-ms hyperpolarizing voltage steps. The amplitude of I_{Na} was measured as the peak inward current with respect to the zero current level. The amplitude of I_{Ca} was the difference between the peak inward current and the current at the end of the test pulse. Reduction of both I_{Ca} and I_K with time ("rundown") was observed initially after rupture of the membrane patch. The rundown phenomenon was more prominent during the initial 3-8 min access of the patch pipette to the interior of the cell with no significant change over 30 min thereafter. When I_{Ca} (evoked at 0 mV) was normalized to the value at 1 min after disruption of membrane patch, it decreased to 83±3, 73±4, 68±4, 69±5, and 67±5% (*n*=11) during the subsequent 3, 6, 9, 12, and 18 min, respectively. Similarly, I_K tail current (evoked at +60 mV) decreased to 84±4, 72±4, 69±3, 68±5, and 69±6% (*n*=13) during the subsequent 3, 6, 9, 12, and 18 min, respectively. Therefore, experiments were performed only on those cells with stable I_{Ca} or I_K 10 min after cell rupture. Current recordings were filtered at 10 kHz bandwidth and then sampled at 100 kHz and stored on the hard disk of an IBM-AT-compatible computer using an on-line data acquisition program (Clampex, pCLAMP). The data were analyzed using a pCLAMP software (Clampfit).

Solutions and drugs

The normal Tyrode solution contained (in mM): NaCl 137, KCl 5.4, $MgCl_2$ 1.1, $NaHCO_3$ 11.9, NaH_2PO_4 0.33, $CaCl_2$ 1.8 and dextrose 11. The HEPES-buffered Tyrode solution contained (in mM): NaCl 137, KCl 5.4, KH_2PO_4 1.2, $MgSO_4$ 1.22, $CaCl_2$ 1.8,

dextrose 22, and HEPES 6, titrated to pH 7.4 with NaOH. The modified KB medium contained (in mM): taurine 10, KCl 25, KH_2PO_4 10, glutamate 70, EGTA 0.5, and dextrose 22, titrated to pH 7.4 with KOH. The internal pipette filling solution contained (in mM): aspartic acid 120, KCl 20, $MgCl_2$ 1, K_2ATP 5, sodium creatine phosphate 5, NaGTP 0.2, EGTA 5, and HEPES 10, adjusted to pH 7.2 with KOH. The Cs^+-containing pipette solution contained (in mM): CsCl 130, EGTA 5, tetraethylammonium (TEA) chloride 15, dextrose 5, and HEPES 10, adjusted to pH 7.2 with CsOH. HA-7 was synthesized by our co-investigators Professors S.C. Kuo and T.P. Lin. Adenosine, tetrodotoxin (TTX), nifedipine, E4031 dihydrochloride and all the chemicals of the physiological solution were purchased from Sigma-Aldrich. (-)-[3*R*, 4*S*]-chromanol 293B (*N*-[(3*R*, 4*S*)-6-Cyano-3,4-dihydro-3-hydroxy-2,2-dimethyl-2*H*-1-benzopyran-4-yl]-*N*-methylethanesufonamide) was purchased from Tocris Chem. Co. (Ellisville, MO, U.S.A.). d-Sotalol hydrochloride was a gift from Bristol-Myers-Squibb. HA-7, nifedipine, d-sotalol and chromanol 293B were dissolved in dimethylsulfoxide (DMSO). Other drugs were dissolved in physiological saline before the start of the experiment. In control experiments, the final concentration of DMSO up to 0.1% produced no significant effect on muscle contractions and electrophysiological parameters of the cells. HA-7 was dissolved in 100% DMSO as a stock solution of the highest concentration of 0.2 M. Final concentrations (0.1, 0.3, 1, 3, 10, 30, and 100 μM) of HA-7 were obtained by cumulative adding aliquots of corresponding stock solutions (1, 2, 10, 20, 50, 200, and 200 mM) to the physiological or external solutions to limit the final concentration of DMSO to about 0.096%. All the stock solutions of d-sotalol, an agent with better solubility, were dissolved in 50% DMSO with distilled water. When stock solutions (the highest concentration was 0.2 M) of d-sotalol were given in a cumulative manner to obtain each final concentration from 3 to 300 μM, the total amount of DMSO approximated to 0.087%. During the

antiarrhythmic experiments, we used stock solutions with different concentrations to obtain an identical final vehicle (DMSO) concentration of 0.06%.

Data analysis

Statistical analysis was made using an analysis of variance (ANOVA) for repeated measures with Dunnett's *t* test for multiple comparisons. Incidences of arrhythmias were compared by a χ^2 procedure followed by pairwise comparison by use of a Fisher's exact test. With the exception of incidences of arrhythmias, all the data are expressed as means ± s.e.m. Differences at a $P<0.05$ level were considered statistically significant. Concentration-response curves were fitted by an equation of the form:

$$E = E_{max}/[1+(IC_{50}/C)^{n_H}]$$

where E is the effect at concentration C, E_{max} is maximal effect, IC_{50} is the concentration for half-maximal block and n_H is the Hill coefficient.

Results

Modification of the electrophysiological properties of the cardiac conduction system. Intracardiac recording detected the atrial activity, His potential, and ventricular activity (Fig. 1). Changes in the electrophysiological parameters of the cardiac conduction system in guinea pig hearts after application of HA-7 and d-sotalol are summarized in Table 1. The basic cycle length (BCL) was significantly lengthened by HA-7 at a low concentration (10 μM) and this effect was concentration-dependent. At higher concentrations (≧ 30 μM), the conduction through the AV node (AH interval) and the AV nodal Wenckebach cycle length and refractory period were prolonged. Additionally, HA-7 prolonged the atrial refractory period at a concentration of 30 μM or higher. At higher concentrations (100 μM), the ventricular repolarization time (VRT) was also prolonged. The conduction interval through the atrial tissue (SA interval) and the His-Purkinje system (HV) were not significantly affected. In the present experimental protocol the AV node usually became refractory to premature extrastimulation before the His-Purkinje system became refractory. Therefore, only the functional refractory period of the His-Purkinje system (shortest conducted V_1V_2 interval) was measured. This was significantly prolonged by HA-7 at a concentration of 30 μM or higher. As compared with HA-7, d-sotalol caused less significant effects on the atrial, AV nodal and His-Purkinje system parameters but comparable or greater effects on BCL and VRT. Both HA-7 and d-sotalol tended to prolong the refractory period of the ventricle though this change did not reach statistical significance. The effect of d-sotalol on some of the parameters only partially reversed during the 60 min washout.

The atrial cycle length-response relations for the negative dromotropic effects (figure not shown) indicated that prolongation of the AH conduction interval caused by HA-7 was

greater at faster atrial pacing rates than at slower rates. Such frequency-dependent effects on the AV node could also be observed in the d-sotalol treatment group. HA-7 at 100 μM prolonged the AH interval from 64±2 to 80±4 ms (P<0.01, n=9) and from 66±2 to 92±5 ms (P<0.001, n=9) at atrial cycle lengths of 300 ms and 260 ms, respectively. Eqimolar d-sotalol prolonged this parameter from 56±2 to 68±4 ms (P<0.05, n=8) and from 58±2 to 85±10 ms (P<0.01, n=8) at atrial cycle lengths of 300 ms and 260 ms, respectively.

Antiarrhythmic testing in isolated hearts. In the reperfusion-induced VF model, one group of hearts was used as a vehicle control (0.06% DMSO) group while the other two groups were exposed to either HA-7 or d-sotalol (30 and 100 μM). Arrhythmia induced by reperfusion of the globally ischaemic heart appeared within 10-30 sec. There was no significant difference in both the incidence and duration of VF for either compound at 30 μM as compared with vehicle controls (Table 2). When the drug concentration was increased to 100 μM, the incidence of VF was significantly reduced in HA-7 but not in d-sotalol group, while the VF duration was significantly reduced in both groups. Also, HA-7 caused a more prominent shortening of mean duration of VF than that of d-sotalol.

In the control condition, AF could not be induced by a train of stimuli at an intensity up to 14 mA in Langendorff-perfused hearts. After the application of 20 μM adenosine, AFT was decreased to about 1.5 mA, which was associated with a marked decrease in AERP (Table 3). Addition of 100 μM HA-7 significantly increased AFT and reversed the adenosine-induced decrease in ERP. Our unpublished data showed that this later effect might not be mediated by blockade of the adenosine receptor. In contrast, the vehicle or d-sotalol had no apparent effect on AFT (Table 3).

Effects of HA-7 on action potentials and contractile force in atrial strips. The effects of HA-7 (30 and 100 μM) superfusion on the action potential in a left atrial strip paced at 1

JPET Fast Forward. Published on September 20, 2005 as DOI: 10.1124/jpet.105.092106
This article has not been copyedited and formatted. The final version may differ from this version.

Hz are shown in Fig. 2a (left panel). HA-7 at 100 μM significantly lengthened the action potential durations measured both at 50% and 90% of repolarization (APD_{50} and APD_{90}) from 36±2 to 48±3 ms (P<0.05, ANOVA, n=8) and from 82±5 to 102±5 ms (P<0.05, n=8), respectively, without causing considerable change in the resting membrane potential (RMP) (control mean value = –79±2 mV) and the action potential amplitude (APA) (control = 108±1 mV). At the same time, HA-7 (100 μM) caused a significant decrease in the maximal rate of depolarization (V_{max}) from 163±7 to 134±7 V/s (P<0.05, n=8). Concurrent with a prolongation of APD, HA-7 (30 and 100 μM) produced an increase in contractile force (CF) (figure not shown) to 160±6% (P<0.001, n=8) and 246±18% (P<0.01, n=8) of the control, respectively. In contrast, d-sotalol had no apparent effect on the action potential parameters and CF in atrial strips at any of the concentrations (10–100 μM) studied. Typical action potential tracings before and after treatment with 100 μM d-sotalol were shown in the right panel of Fig. 2a. The APD_{50}, APD_{90}, and V_{max} values before treatment were 27±2 ms, 67±3 ms, and 136±8 V/s (n=10) and these values were changed to 31±4 ms, 76±4 ms, and 135±11 V/s, respectively (all P>0.05, n=10) after treatment with 100 μM d-sotalol. The same concentration of d-sotalol only caused a small increase in CF to 107±6% (P>0.05, n=10) of the control.

Effects of HA-7 on action potentials and contractile force in papillary muscles. In papillary muscles paced at 1 Hz, HA-7 at 100 μM caused a moderate but insignificant increase in contractile force (155±17% of the control) (figure not shown) and prolongation of APD_{90} (from 186±5 ms to 201±6 ms, n=9) (Fig. 2b, left panel). The higher concentrations of HA-7 (150 μM) caused a further increase in CF to 183±29% of the control value (P<0.01, n=9) accompanied by a significant prolongation of APD_{90} from 186±5 ms to 205±5 ms (P<0.05, n=9). HA-7 had a tendency to decrease V_{max} though this effect did not reach

statistical significance. At higher concentrations up to 150 μM, HA-7 decreased the V_{max} from 189±9 to 163±14 V/s (P>0.05, n=9). HA-7 produced little change in the RMP (control = –87±1 mV), APA (control = 122±1 mV), APD_{25} or APD_{50} (control = 157±4 ms) although there was a trend for APD_{25} to be shortened slightly (from 103±4 to 95±4 ms at 150 μM). Despite the small effect on left atrial action potentials, d-sotalol had a marked effect on APD of papillary muscles at a stimulation frequency of 1 Hz (Fig. 2c, left panel). d-Sotalol at 100 μM significantly lengthened the APD_{50} and APD_{90} from 149±4 to 181±5 ms (P<0.001, n=8) and from 175±4 to 213±4 ms (P<0.001, n=8), respectively. d-Sotalol did not affect the RMP, APA, V_{max} or APD_{25} (data not shown). Unlike the positive inotropy produced by HA-7, d-sotalol produced little change in CF as previously reported by Yang et al. (1992). d-Sotalol at 100 μM caused a slight decrease in CF to 81±4% (P>0.05, n=8) of the control.

Frequency-dependent effects of HA-7. To investigate whether HA-7 can exert any use- or frequency-dependent action, we also studied its effects at different stimulation frequencies in papillary muscles. Stimulation frequency was increased sequentially to 0.1, 0.5, 1, 2 and 3 Hz (3 min each), and the steady-state action potentials were recorded before and during the application of HA-7 (30-150 μM) and d-sotalol (10-100 μM). Typical action potential tracings obtained at driven rates of 1 and 3 Hz before and after treatment with 100 μM HA-7 and d-sotalol are shown in Fig. 2b and c, respectively. The results for the changes of APD_{90} are shown in Fig. 3. In untreated control groups, when the stimulation frequency was changed from 0.1 to 3 Hz, the APD initially slightly increased and then decreased (Fig. 3a and b) while the other parameters, RMP, APA, and V_{max}, were not changed significantly (data not shown). The prolonging effect of HA-7 on APD_{90} was similar throughout the pacing frequency range (Fig. 3a and c), that is, it did not show true frequency dependence. At a stimulation frequency of 3 Hz, HA-7 (100 and 150 μM) significantly lengthened the APD_{90} from 140±5 ms to

JPET Fast Forward. Published on September 20, 2005 as DOI: 10.1124/jpet.105.092106
This article has not been copyedited and formatted. The final version may differ from this version.

158±5 ms (P<0.05, n=9) and 161±5 ms (P<0.05, n=9), respectively. In contrast, d-sotalol (≧ 30 μM) caused greater prolongation of APD_{90} at lower pacing frequencies (from 0.1 to 1 Hz) than at higher frequencies (Fig. 3b and d), indicating the reverse frequency dependent effect on APD is similar to previous reports (Schmitt et al., 1991). At 3 Hz pacing rate, 100 μM d-sotalol only slightly prolonged the APD_{90} from 115±7 to 132±9 ms (P>0.05, n=8).

Effects of HA-7 on delayed outward K^+ current (I_K). In mammalian species, I_K consists of the rapid and slow components, I_{Kr} and I_{Ks}, respectively (Sanguinetti and Jurkiewicz, 1990; Li et al., 1996). To record I_K, the membrane potential of myocytes was held at –40 mV to inactivate I_{Na} and subsequently depolarized by pulses lasting either 3000 ms (I_{Ks}) or 250 ms (I_{Kr}). Test potentials of depolarization varied between 0 and +60 mV for I_{Ks} but between –20 and +50 mV for I_{Kr}. The membrane was then repolarized to –40 mV to record deactivating tail current.

Figure 4a shows superimposed current traces in response to various depolarizing voltage steps under control conditions and during exposure to and after washout of 3 μM HA-7. HA-7 decreased the amplitude of activation currents and the tail currents of I_{Ks}. Average current-voltage (I-V) relationships for the activation currents and the tail currents recorded before and after additions of 1, 3, and 10 μM HA-7 are shown in Fig. 4b and c, respectively. Figure 5a shows sample current traces, corresponding to the labeled measurements depicted in Fig. 5b, obtained before, during, and after cumulative application of 3, 10 and 30 μM HA-7. Figure 5b is a plot that indicates the time course of the changes in the magnitude of I_{Ks} tail current; this protocol was imposed on the cell every 60 seconds. From experiments similar to those shown in Fig. 5a, we derived the concentration-response relation for the inhibition of tail current (Fig. 5d) in which the data are expressed as % inhibition of predrug tail amplitude after step depolarizations to +60 mV. HA-7 decreased $I_{Ks,tail}$ in a concentration-dependent manner.

JPET Fast Forward. Published on September 20, 2005 as DOI: 10.1124/jpet.105.092106
This article has not been copyedited and formatted. The final version may differ from this version.

Under control conditions (in the presence of E4031), the mean $I_{Ks,tail}$ density was 3.2±0.8 pA/pF (*n*=8). The overall data were well described by the Hill equation with a mean IC_{50} of 4.8±1.7 μM, a coefficient of 0.85±0.10, and a maximal inhibition of 103±5 % (*n*=8). In comparison with HA-7, d-sotalol produced less effect on I_{Ks} (Fig. 5c and d). HA-7 also inhibited the I_{Ks} currents of atrial myocytes (Fig. 7a and c). The mean amplitude of $I_{Ks,tail}$ in atrial myocytes elicited at the test potential of +60 mV was 2.7±0.6 pA/pF (*n*=8). The averaged IC_{50} for the effect of HA-7 on $I_{Ks,tail}$ was 3.0±1.1 μM with a maximal inhibition of 99±3% (n_H=0.84±0.09, *n*=8).

Figure 6 depicts that HA-7 could also suppress the I_{Kr} currents in guinea pig ventricular myocytes. The superimposed I_{Kr} current traces before and during exposure to and following washout of 1 μM HA-7 are shown in Fig. 6a. I_{Kr} tail current density-voltage relationships are plotted in Fig. 6b, for control and after application of 0.3, 1 and 3 μM HA-7. Concentration-dependent inhibition of HA-7 on I_{Kr} evoked at a test potential of +30 mV was plotted in Fig. 6d. Under control conditions (in the presence of chromanol 293B), the mean I_{Kr} density was 0.15±0.02 pA/pF (*n*=6). The overall data are well described by the Hill equation with a mean IC_{50} of 1.1±0.3 μM, a coefficient of 1.02±0.14, and a maximal inhibition of 104±3% (*n*=6). d-Sotalol also showed a comparable inhibitory effect on the I_{Kr} current (Fig. 6c and d). The calculated IC_{50} for the effect of d-sotalol on $I_{Kr,tail}$ was 1.7±0.4 μM with a maximal inhibition of 107±2% (n_H=1.01±0.12, *n*=7). In addition, HA-7 also significantly inhibited I_{Kr} in atrial myocytes (Fig. 7b and d). The mean $I_{Kr,tail}$ density in atrial myocytes was 0.44±0.05 pA/pF (n=6). The calculated IC_{50} for the effect of HA-7 on $I_{Kr,tail}$ was 2.1±0.8 μM with a maximal inhibition of 114±6% (n_H=0.77±0.17, *n*=6).

Effect of HA-7 on inward rectifier K^+ current (I_{K1}). I_{K1} was elicited by 200-ms long voltage pulses to potentials between –120 and –10 mV in 10 mV increments from a holding

potential of –80 mV at a stimulation frequency of 0.1 Hz. Each step was preceded by a prestep to –40 mV for 200 ms to inactivate I_{Na}. Figure 8a gives representative current records from a ventricular myocyte in control and after 5 min of exposure to 30 μM HA-7. Steady-state current densities at the end of the test pulse are plotted in Fig. 8b, for control and after superfusion of increasing concentrations of HA-7 (1, 3, 10, and 30 μM) respectively. The resultant I-V relations had relationships typical of I_{K1}-V relations, and both inward- and outward-directed currents were diminished by HA-7 in a concentration-dependent manner. At the test potential of –40 mV and –120 mV, 30 μM HA-7 reduced I_{K1} density from the control value of 8.4±2.7 and –35.7±4.1 pA/pF to 4.3±1.3 (P<0.05, n=6) and –21.2±2.9 pA/pF (P<0.05, n=6), respectively. In contrast, d-sotalol did not change either the inward or outward I_{K1} currents even over the concentration range higher than those of HA-7 (figure not shown). The I_{K1} density at the test potential of –120 mV before and after application of 10, 30, 100 and 300 μM d-sotalol were –40.1±3.8, –41.0±3.8, –40.2±3.3, –38.3±3.8, and –36.3±4.1 pA/pF (n=6), respectively.

Effects of HA-7 on inward Na^+ (I_{Na}) and L-type Ca^{2+} (I_{Ca}) currents. I_{Na} was elicited every 30 seconds with a step depolarization from -80 to -20 mV. Figure 9ai shows the superimposed current traces from typical experiments with 1 and 3 μM HA-7. Concentration-dependent inhibition of HA-7 on I_{Na} was shown in Fig. 9aii. Under control conditions, the mean I_{Na} density was 52.1±5.1 pA/pF (n=9). The calculated IC_{50} was 2.9±0.6 μM with a maximal inhibition of 108±3% (n_H=1.44±0.23, n=9). Compared with HA-7, peak I_{Na} was decreased by 2±5, 17±7, 30±8, 35±9, and 45±12% (n=9) after 3, 10, 30, 100 and 300 μM d-sotalol, respectively. HA-7 also inhibited the I_{Na} currents of atrial myocytes. Peak I_{Na} was decreased by 26±5, 69±4, and 92±3% (n=5) after 1, 3, and 10 μM HA-7, respectively.

L-type Ca^{2+} current (I_{Ca}) was recorded every 10 seconds during a 300-ms long

depolarizing test pulses ranging from –40 to +50 mV. Representative superimposed current traces evoked at 0 mV under control conditions, after treatment with 10 μM HA-7, and after washout, are shown in the inset in Fig. 9bii. Figure 9bi shows the effects of 1 and 3 μM HA-7 on the peak I-V relationship. HA-7 reduced peak current amplitude in a concentration-dependent manner but did not alter the shape of the I-V relationships. Figure 9bii shows the concentration-response curve for the effect of HA-7 on the peak I_{Ca}. Average control peak current amplitude at 0 mV was 7.9±1.1 pA/pF (*n*=8). From these data an IC_{50} value of 4.0±1.5 μM and a maximum inhibition of 69±7% were obtained with a Hill slope of 1.12±0.14 (*n*=8). In comparison with HA-7, d-sotalol at 3, 10, 30, 100 and 300 μM decreased I_{Ca} by 4±5, 11±11, 28±8, 37±9, and 51±13% (*n*=8), respectively. HA-7 also moderately inhibited the I_{Ca} currents of atrial myocytes. Peak I_{Ca} was only decreased by 18±6, 34±8, and 49±10% (*n*=5) after 1, 3, and 10 μM HA-7, respectively.

Discussion

The major findings from this study are as follows: (1) HA-7 prolonged conduction intervals and the refractoriness of the cardiac conduction system, (2) HA-7 lengthened the repolarization in both atrial and ventricular muscles, (3) HA-7 exhibited a lack of reverse frequency-dependent prolongation of APD, (4) HA-7 was more effective than d-sotalol in reducing experimental atrial and ventricular arrhythmias, (5) HA-7 exerted equipotent I_{Kr} blocking activity as d-sotalol but was more potent on I_{Ks}, I_{K1}, I_{Na}, and I_{Ca}. Using a typical class III agent d-sotalol as a reference compound, the results of this study demonstrate that a non-selective ion channel blocker HA-7 was more effective in modifying electrophysiological parameters in atrial and ventricular tissue and, by virtue of these changes, HA-7 may possess a higher antiarrhythmic effectiveness than d-sotalol in guinea pig heart.

In this study, the experimental AF could be easily induced by a high frequency atrial stimulation with low intensity during adenosine perfusion in isolated guinea pig hearts. The shortening of ERP resulting from the activation of $I_{K(Ado)}$ and the subsequent shortening of APD by adenosine (Watanabe et al., 1996) likely underlies the induction of AF in this study. The dominant mechanism of this atrial arrhythmia is considered to be reentry (Nattel, 2002). In general, drugs that lengthen the cardiac APD and refractoriness (i.e., class III agents) should prevent premature excitation of cardiac cells and should suppress the incidence of re-entrant tachyarrhythmias, such as atrial and ventricular fibrillation (Singh and Nademanee, 1985). Our study has shown that higher concentrations of HA-7 reverted the shortened atrial ERP caused by adenosine toward control levels. The improved suppressive effect of HA-7 compared with d-sotalol on experimental AF in the present model is correlated with the more prominent increase of AERP and atrial APD by HA-7.

The mechanism(s) underlying the genesis of the ischaemia/reperfusion-induced lethal

arrhythmias (VT and VF) are complex but a number of factors have been implicated as potential culprits. These detrimental factors, which mostly occur during early reperfusion, may include the formation of oxygen free radicals, the heterogeneity of tissue injury and recovery, and the subsequent electrophysiological disturbances including the reentry and enhanced automaticity such as oscillatory afterpotentials (Manning and Hearse, 1984; Pogwizd and Corr, 1987). In the reperfusion-induced arrhythmia model, HA-7 was applied from the pre-ischaemic through the reperfusion period and might cause some pharmacological effects over this period so that could promptly prevent or ameliorate the arrhythmias which occur early at subsequent reperfusion. The efficacy of HA-7 to reduce both the incidence and mean duration of VF was greater than d-sotalol, perhaps through the prolonging effects on ventricular APD, VRT interval, or VERP. This may suggests that HA-7 may act via a mechanism that includes the prolongation of repolarization and the subsequent suppression of reentry-induced ventricular tachyarrhythmias. Additionally, through the blockade of I_{Na} and I_{Ca}, HA-7 may reduce the influx of these ions and, as such, help to suppress the occurrence of oscillatory afterpotentials or extrasystoles provoked by Ca^{2+} overload during ischemia and reperfusion. Moreover, in contrast to the inherent reverse frequency-dependent effect of d-sotalol that may attenuate its action during conditions of high frequency cardiac rhythm such as VT or VF, the lack of reverse frequency-dependent effect of HA-7 may maintain its antiarrhythmic action in the same conditions.

The balance between plateau inward and outward currents determines the APD. In this study, it is highly possible that the prolongation of APD in atrial and papillary muscles by HA-7 may be related to its inhibition on I_K (i.e., I_{Kr} and I_{Ks}) although a slight reduction of outward I_{K1} current may also contribute to APD prolongation. Since HA-7 also inhibited I_{Ca}, this effect may counterbalance the inhibition of outward currents which could explain the

JPET Fast Forward. Published on September 20, 2005 as DOI: 10.1124/jpet.105.092106
This article has not been copyedited and formatted. The final version may differ from this version.

slightly shortening of APD_{25} of papillary muscle. Similar to previous observations (Carmeliet, 1985; Malécot and Argibay, 1999), d-sotalol was found to prolong APD via inhibition of K^+ outward currents (mainly I_{Kr}) in this study. With respect to the effect on APD, d-sotalol exhibits greater potency on guinea pig ventricular fibres than on atrial fibres. Similar difference in tissue sensitivity was noted in early study reported by Campbell (1987). Since I_K is largely responsible for repolarization in sinus node fibres (Schram et al., 2002), it is reasonable to speculate that both HA-7- and d-sotalol-induced bradycardiac effects are due to inhibition of I_K in the sinus node and that inhibition of I_{Ca} by HA-7 may also play a part. However, further studies are required to determine the direct effects of HA-7 on this preparation.

HA-7 moderately prolonged ventricular APD_{90} at low and high heart rates while the effect of d-sotalol was largely attenuated at fast rates. This property of d-sotalol is similar to earlier data on most class III antiarrhythmic agents (Katritsis and Camm, 1993). This reverse frequency-dependent effect (Hondeghem and Snyders, 1990) may leads to an increase in the dispersion of repolarization and favor the occurrence of cardiac arrhythmias. Jurkiewicz and Sanguinetti (1993) proposed that the reverse frequency-dependent effect on APD of typical class III agents is a consequence of selective blockade of I_{Kr}. It has been suggested that I_{Ks} accumulation at increased frequencies decreases the relative importance of I_{Kr}, reducing the impact of I_{Kr} blockade on APD prolongation (Jurkiewicz and Sanguinetti, 1993). They suggested that compounds that inhibit I_{Ks} might be devoid of reverse use-dependence. Actually, it has been shown that an agent that blocks both components of I_K might have a more consistent effect on action potentials at different rates and an improved safety profile over a specific I_{Kr} blocker (Sager et al., 1993). In this study, as compared with d-sotalol that blocked I_{Kr} selectively, HA-7 inhibited both I_{Kr} and I_{Ks}, so, it is possible that the lack of

reverse use-dependent effect of HA-7 may arise from its non-selective blockade of both I_K components. However, other mechanisms, as will be discussed later or yet to be identified, may also play some role.

Our study demonstrated that HA-7 decreased the V_{max} value of the atria and to a lesser extent, the ventricular papillary muscles in a concentration-dependent manner. This effect is consistent with the inhibition of the I_{Na} by this agent which likely contributes to the antiarrhythmic and AERP and HPFRP prolongation actions by this agent. In rat ventricular myocytes, our previous report showed that HA-7 exerted use-dependent inhibition on I_{Na} and may bind preferentially to the inactivated state of Na^+ channels (Su et al., 1997). In this context, the greater V_{max} suppressing effect of HA-7 in atria than in papillary muscles may be explained by the less negative resting membrane potential and more prominent drug-induced APD prolongation of atrial tissues. Because of such properties, atrial tissues would have higher ratio of inactivated Na^+ channels that may enhance the channel blockade action of HA-7. In addition, the use-dependent inhibition on I_{Na} may also be expected to confer the greater suppressive actions on atrial or ventricular tachyarrhythmias of HA-7 than d-sotalol.

In keeping with the greater frequency-dependently depressant effects on the AV nodal conduction (i.e., A-H interval lengthening), HA-7 caused a greater prolongation of the WCL and AVNERP than d-sotalol. These actions may be mainly related to its Ca^{2+} channel blockade activity. However, the inhibition of K^+ channels may also contribute to the prolongation of AVNERP. The prolongation of A-H interval, AV nodal ERP, and WCL by HA-7 at shorter atrial cycle lengths indicates that the negative dromotropic effect of this drug became greater as the atrial rate increased. Drugs that exacerbate the physiological frequency-dependent modulatory effects of atrial rate on AV nodal conduction delay (Meijler et al., 1996) provide additional protection against excessive ventricular rate during rapid atrial fibrillation

or flutter (Ganz and Friedman, 1995). In this study, HA-7 exerted efficacy against experimental atrial arrhythmias. However, whether or not HA-7 could also filter the atrial impulse and control the ventricular rate during rapid atrial arrhythmias through AV nodal suppression remains to be established.

In conclusion, HA-7 possessed a multiple K^+, Na^+ and Ca^{2+} currents-blocking profile without reverse frequency dependence in guinea pig heart preparations. The antiarrhythmic efficacy on either electrically induced AF or reperfusion-induced VF in guinea pig heart was greater than that of a typical class III agent d-sotalol. It is well known that patients with ischaemic heart disease are particularly susceptible to events of atrial or ventricular tachyarrhythmias and that the later may even culminate in sudden death. Our findings suggest that HA-7 may be useful for the prevention of such arrhythmias associated with ischaemic heart disease. The modest positive inotropy by HA-7 may be viewed as a potential therapeutic advantage over d-sotalol and other similar cardiodepressant agents. Furthermore, it has been suggested that block of I_{Ca} and/or I_{Na}, by reducing the risk of EAD development with excessive APD prolongation, attenuating excessive repolarization delay and temporal dispersion of repolarization may contribute to the reduced proarrhythmic potential of the multiple channel blockers (Abrahamsson et al., 1996; Amos et al., 2001). Consequently, because of its multifaceted actions, it can be reasonably expected that HA-7 may possess promising antiarrhythmic efficacy but fewer or negligible proarrhythmic risk.

Acknowledgements

The authors thank Ms. Chin-Mei Kuo and Ms. Miao-Sui Lin for technical assistance. The authors also gratefully acknowledge Bristol-Myers-Squibb for providing d-sotalol.

References

Abrahamsson C, Carlsson L, and Duker G (1996) Lidocaine and nisoldipine attenuate almokalant-induced dispersion of repolarization and early afterdepolarizations in vitro. *J Cardiovasc Electrophysiol* **7:**1074-1081.

Amos GJ, Abrahamsson C, Duker G, Hondeghem L, Palmer M, and Carlsson L (2001) Potassium and calcium current blocking properties of the novel antiarrhythmic agent H 345/52: implications for proarrhythmic potential. *Cardiovasc Res* **49:**351-360.

Bosch RF, Gaspo R, Busch AE, Lang HJ, Li GR, and Nattel S (1998) Effects of the chromanol 293B, a selective blocker of the slow, component of the delayed rectifier K^+ current, on repolarization in human and guinea pig ventricular myocytes. *Cardiovasc Res* **38:**441-450.

Campbell TJ (1987) Cellular electrophysiological effects of D- and DL-sotalol in guinea-pig sinoatrial node, atrium and ventricle and human atrium: differential tissue sensitivity. *Br J Pharmacol* **90:**593-599.

Carmeliet E (1985) Electrophysiologic and voltage clamp analysis of the effects of sotalol on isolated cardiac muscle and Purkinje fibers. *J Pharmacol Exp Ther* **232:**817-825.

Chang GJ, Su MJ, Hung LM, and Lee SS (2002) Cardiac electrophysiologic and antiarrhythmic actions of a pavine alkaloid derivative, O-methyl-neocaryachine, in rat heart. *Br J Pharmacol* **136:**459-471.

Echt DS, Liebson PR, Mitchel LB, Peters RW, Obias-Manno D, Barker AH, and The CAST Investigators (1991) Mortality and morbidity in patients receiving encainide, flecainide, or placebo. The Cardiac Arrhythmia Suppression Trial. *N Engl J Med* **324:**781-788.

Ganz LI and Friedman PL (1995) Supraventricular tachycardia. *N Engl J Med* **332:**162-173.

Hamill OP, Marty A, Neher E, Sakmann B, and Sigworth FJ (1981) Improved patch-clamp techniques for high resolution current recording from cells and cell-free membrane patches. *Pflügers Arch* **391:**85-100.

Hohnloser SH and Woosley RL (1994) Sotalol. *N Engl J Med* **331:**31-38.

Hondeghem LM and Snyders DJ (1990) Class III antiarrhythmic agents have a lot of potential but a long way to go. Reduced effectiveness and dangers of reverse use dependence. *Circulation* **81:**686-690.

Hume JR and Uehara A (1985) Ionic basis of the different action potential configurations of single guinea-pig atrial and ventricular myocytes. *J Physiol* **368:**525-544.

Isenberg G and Klöckner U (1982) Calcium tolerant ventricular myocytes prepared by preincubation in a "KB medium". *Pflügers Arch* **395:**6-18.

Josephson IR, Sanchez-Chapula J, and Brown AM (1984) Early outward current in rat ventricular cells. *Circ Res* **54:**157-162.

Jurkiewicz NK and Sanguinetti MC (1993) Rate-dependent prolongation of cardiac action potentials by a methanesulfonanilide class III antiarrhythmic agent. Specific block of rapidly activating delayed rectifier K^+ current by dofetilide. *Circ Res* **72:**75-83.

Kabell G, Buchanan LV, Gibson JK, and Belardinelli L (1994) Effects of adenosine on atrial refractoriness and arrhythmias. *Cardiovasc Res* **28:**1385-1389.

Katritsis D and Camm AJ (1993) New class III antiarrhythmic drugs. *Eur Heart J* **14:**93-99.

Li GR, Feng J, Yue L, Carrier M, and Nattel S (1996) Evidence for two components of delayed rectifier K^+ current in human ventricular myocytes. *Circ Res* **78:**689-696.

Malécot CO and Argibay JA (1999) Block of gating currents related to K^+ channels as a mechanism of action of clofilium and d-sotalol in isolated guinea-pig ventricular heart cells. *Br J Pharmacol* **128:**301-312.

Manning AS and Hearse DJ (1984) Reperfusion-induced arrhythmias: mechanism and prevention. *J Mol Cell Cardiol* **16:**497-518.

Mátyus P, Varro A, Papp GJ, Wamhoff H, Varga I, and Virág L (1997) Antiarrhythmic agents: current status and perspectives. *Med Res Rev* **17:**427-451.

Meijler FL, Jalife J, Beaumont J, and Vaidya D (1996) AV nodal function during atrial fibrillation: the role of electrotonic modulation of propagation. *J Cardiovasc Electrophysiol* **7:**843-861.

Nattel S (2002) New ideas about atrial fibrillation 50 years on. *Nature* **415:**219-226.

Pogwizd SM and Corr PB (1987) Electrophysiologic mechanisms underlying arrhythmias due to reperfusion of ischemic myocardium. *Circulation* **76:**404-426.

Sager PT, Uppal P, Follmer C, Antimisiaris M, Pruitt C, and Singh BN (1993) Frequency-dependent electrophysiologic effects of amiodarone in humans. *Circulation* **88:**1063-1071.

Sanguinetti MC and Bennett PB (2003) Antiarrhythmic drug target choices and screening. *Circ Res* **93:**491-499.

Sanguinetti MC and Jurkiewicz NK (1990) Two components of cardiac delayed rectifier K^+ current. Differential sensitivity to block by class III antiarrhythmic agents. *J Gen Physiol* **96:**195-215.

Schmitt C, Brachmann J, Karch M, Waldecker B, Navarrete L, Montero M, Beyer T, and Kubler W (1991) Reverse use-dependent effects of sotalol demonstrated by recording

monophasic action potentials of the right ventricle. *Am J Cardiol* **68:**1183-1187.

Schram G, Pourrier M, Melnyk P, and Nattel S (2002) Differential distribution of cardiac ion channel expression as a basis for regional specialization in electrical function. *Circ Res* **90:**939-950.

Singh BN and Nademanee K (1985) Control of cardiac arrhythmias by selective lengthening of repolarization: theoretic considerations and clinical observations. *Am Heart J* **109:**421-430.

Su MJ, Chang GJ, Wu MH, and Kuo SC (1997) Electrophysiological basis for the antiarrhythmic action and positive inotropy of HA-7, a furoquinoline alkaloid derivative, in rat heart. *Br J Pharmacol* **122:**1285-1298.

Tamargo J, Caballero R, Gómez R, Valenzuela C, and Delpón E (2004) Pharmacology of cardiac potassium channels. *Cardiovasc Res* **62:**9-33.

van der Hooft CS, Heeringa J, van Herpen G, Kors JA, Kingma JH, and Stricker BHC (2004) Drug-induced atrial fibrillation. *J Am Coll Cardiol* **44:**2117-2124.

Waldo AL, Camm AJ, deRuyter H, Friedman PL, MacNeil DJ, Pauls JF, Pitt B, Pratt CM, Schwartz PJ, and Veltri EP (1996) Effect of d-sotalol on mortality in patients with left ventricular dysfunction after recent and remote myocardial infarction. The SWORD Investigators. Survival With Oral d-Sotalol. *Lancet* **348:**7-12.

Watanabe Y, Hara Y, Tamagawa M, and Nakaya H (1996) Inhibitory effect of amiodarone on the muscarinic acetylcholine receptor-operated potassium current in guinea pig atrial cells. *J Pharmacol Exp Ther* **279:**617-624.

Yang T, Tnade PM, and Refsum H (1992) Electromechanical action of dofetilide and D-

sotalol during simulated metabolic acidosis in isolated guinea pig ventricular muscle. *J Cardiovasc Pharmacol* **20:**889-894.

Footnotes

This work was supported by grants from the National Science Council (NSC 91-0420-B-002-123) of Taiwan and CMRP 1231 from Chang Gung Medical Research Foundation.

Address correspondence to: **Gwo-Jyh Chang, Ph. D.,**

Graduate Institute of Clinical Medicinal Sciences,

College of Medicine,

Chang Gung University,

5 Fu-Shing St, Kwei-Shan,

Tao-Yuan, Taiwan.

E mail: gjchang@adm.cgmh.org.tw

Legends for Figures

Fig. 1 Representative ventricular electrograms recorded at spontaneous sinus rhythm (left panel) and His bundle electrograms recorded during atrial pacing at 300 ms after HA-7 of the guinea pig heart. A: atrial depolarization. H: His bundle depolarization. S: stimulation artifact. T: ventricular repolarization. V: ventricular depolarization.

Fig. 2 Original superimposed tracings showing the effects of HA-7 and d-sotalol on the action potentials in guinea pig left atrial strips driven at 1 Hz (panel a) and ventricular papillary muscles driven at 1 and 3 Hz (panel b and c), respectively. The records were taken under control (CTRL) conditions and after exposure to the corresponding drug concentrations. Drugs were applied in a cumulative manner. For clarity, only the data obtained at 100 μM were shown in panel a (right tracing), b and c. Data at different frequencies were obtained from the same impalement.

Fig. 3 Concentration and frequency dependent effects of HA-7 and d-sotalol on action potential duration at 90% of repolarization (APD_{90}) recorded from papillary muscles. APD_{90} before and during application of HA-7 (a, *n*=9) or d-sotalol (b, *n*=8) was plotted as a function of stimulation frequency. Frequency dependence of APD_{90} was measured at the end of the predrug control period and again after exposure to each drug concentration tested for the cumulative concentration-response curve. (c) and (d): Effects of cumulative increases in HA-7 (*n*=9) and d-sotalol (*n*=8) on percentage change of APD_{90} at 0.1, 0.5, 1, 2 and 3 Hz pacing conditions. Each value represents mean±s.e.m.

Fig. 4 Effects of HA-7 on slow component of the delayed rectifier K^+ current (I_{Ks}) in guinea pig ventricular myocytes. (a) Superimposed current traces obtained during 3-s depolarizing pulses to potentials ranging from 0 to +60 mV in 10-mV steps applied from a holding potential of –40 mV at 0.1 Hz before (control) and during 5-min exposure to 3 μM HA-7 and after washout of the drug. (b) and (c): Average current density-voltage relations for time-dependent activation currents (panel b) and tail currents (panel c) of I_{Ks} recorded under control conditions and during exposure to increasing concentrations of HA-7. Data are expressed as mean±s.e.m. (*n*=8).

Fig. 5 Concentration-related block of I_{Ks} in ventricular myocytes by HA-7 and d-sotalol. (a) Superimposed current traces recorded from a cell before and after cumulative HA-7 treatment. I_{Ks} was activated using depolarizing voltage steps of 3-sec duration clamped from the holding potential of –40 mV to the test potential of +60 mV (protocol inset in top panel). (b) The tail current amplitude is plotted as a function of time during sequential application of HA-7. Letters on the curve correspond to traces in panel a. Sample traces in panel a from one cell were taken four different times: **a**, at the beginning of the experiment (control); **b**, **c**, and **d**, in the presence of 3, 10, and 30 μM HA-7, respectively. (c) Superimposed I_{Ks} current traces recorded before and after cumulative d-sotalol treatment. (d) Concentration-response curve for the inhibition of HA-7 (*n*=8) and d-sotalol (*n*=8) on I_{Ks} tail current. Percentage inhibition of tail current amplitude corresponding to the control value was plotted against drug concentration. Symbols represent mean±s.e.m.. The solid line was drawn by fitting to the Hill equation.

Fig. 6 Effects of HA-7 and d-sotalol on the rapid component of delayed rectifier K^+ current

(I_{Kr}) in ventricular myocytes. (a) Representative recordings of I_{Kr} obtained under control conditions (left panel), in the presence of 1 μM HA-7 (right panel) and upon 8 min of washout (lower left panel). The current was activated by 250 ms long depolarizing voltage pulses from holding potential of –40 mV to various test potentials ranging from –20 to +50 mV in 10-mV increments. (b) Current-voltage relationship of I_{Kr} tail current density under control conditions and in the presence of 0.3, 1 and 3 μM HA-7. Data are given as mean±s.e.m. (*n*=6). (c) Superimposed I_{Kr} current traces evoked at +30 mV recorded before and after cumulative d-sotalol treatment. (d) Concentration-response curve for the blocking effect of HA-7 (*n*=6) and d-sotalol (*n*=7) on I_{Kr} tail current. Symbols represent mean±s.e.m.

Fig. 7 Concentration-dependence of inhibition on I_{Ks} and I_{Kr} in atrial myocytes by HA-7. (a) and (b) Representative superimposed I_{Ks} and I_{Kr} current traces, respectively, generated by the protocol as shown in the upper panels in the absence or presence of HA-7. (c) and (d) Concentration-response curve for the blocking effect of HA-7 on I_{Ks} (*n*=8) and I_{Kr} (*n*=6) tail currents, respectively. Symbols represent mean±s.e.m.

Fig. 8 Effects of HA-7 on inward rectifier K^+ current (I_{K1}) in guinea pig ventricular myocytes. (a) Sample traces used to construct I-V relationships in the absence (control) and after 5-min exposure to 30 μM HA-7. Currents were serially elicited (from –20 to –120 mV for 200 ms in 10 mV steps) after a prepulse of –40 mV. Dashed lines indicate zero current level. (b) Average current density-voltage relationships of steady-state component of I_{K1} in control and after 5-min exposure to 1, 3, 10, and 30 μM HA-7 (*n*=6).

Fig. 9 (a) Effects of HA-7 on sodium inward current (I_{Na}) in guinea pig ventricular myocyte.

(ai) Superimposed current traces of I_{Na} recorded in the control conditions and after exposure to 1 μM and 3 μM HA-7. I_{Na} was elicited by a 30 ms-depolarizing pulse from a holding potential of –80 mV to –20 mV. Dashed lines indicate zero current level. (aii) Concentration-response curve for the inhibition of I_{Na} by HA-7. Symbols represent mean±s.e.m. (*n*=9). (b) Effects of HA-7 on calcium inward current (I_{Ca}) in guinea pig ventricular myocyte. (bi) I-V relationships for I_{Ca} recorded under control conditions and during exposure to 1 and 3 μM HA-7. Currents were elicited during 300 ms depolarizing pulses ranging from –40 mV to +50 mV in 10-mV steps from a holding potential of –40 mV. Symbols represent mean±s.e.m. (*n*=6). (bii) Concentration-response curve for the inhibition of I_{Ca} by HA-7. Symbols represent mean±s.e.m. (*n*=8). Inset shows original recordings of I_{Ca} evoked at 0 mV (holding potential = –40 mV) under control conditions (a), after 5 min exposure to 10 μM HA-7 (b) and after 8 min washout (c). Stimulation frequency was 0.1 Hz. Dashed lines indicate zero current level.

TABLE 1

Concentration-related effects of HA-7 and d-sotalol on the conduction system of guinea pig isolated perfused hearts

Data (in ms) were obtained from 11 (HA-7 group) and 10 (d-sotalol group) experiments and are expressed as mean±s.e.m.

	HA-7 (μM)						d-Sotalol (μM)					
	Control	3	10	30	100	Wash	Control	3	10	30	100	Wash
BCL	312 ± 6	342 ± 10	352 ± 9**	366 ± 9***	400 ± 11***	335 ± 6	309 ± 6	328 ± 5	343 ± 6**	384 ± 7***	411 ± 10***	352 ± 9**
SA	11 ± 1	10 ± 1	12 ± 2	11 ± 1	12 ± 2	13 ± 2	18 ± 1	17 ± 1	19 ± 1	19 ± 1	19 ± 1	19 ± 1
AH	62 ± 2	66 ± 3	70 ± 3	75 ± 4*	88 ± 5***	67 ± 4	56 ± 2	62 ± 3	64 ± 3	65 ± 3	70 ± 4*	72 ± 4**
HV	17 ± 1	19 ± 1	19 ± 1	19 ± 1	20 ± 2	18 ± 1	18 ± 1	21 ± 1	22 ± 1	22 ± 1	23 ± 1	22 ± 1
VRT	177 ± 7	187 ± 7	191 ± 5	195 ± 5	203 ± 6*	182 ± 6	187 ± 4	187 ± 7	198 ± 7	208 ± 6	221 ± 6**	177 ± 6
WCL	186 ± 5	196 ± 7	200 ± 6	216 ± 8*	239 ± 8***	197 ± 7	187 ± 6	202 ± 8	210 ± 8	219 ± 8	226 ± 11*	236 ± 13**
AERP	68 ± 6	78 ± 5	83 ± 5	88 ± 5*	110 ± 6***	74 ± 6	69 ± 5	76 ± 6	77 ± 5	79 ± 5	90 ± 7	74 ± 6
AVNERP	152 ± 5	157 ± 5	166 ± 6	180 ± 7*	223 ± 10***	169 ± 9	154 ± 7	162 ± 7	172 ± 8	183 ± 10	189 ± 7*	211 ± 14*
HPFRP	215 ± 6	228 ± 7	235 ± 7	244 ± 6*	264 ± 10***	234 ± 4	220 ± 8	232 ±10	238 ± 10	240 ± 11	256 ± 12	257 ± 15
VERP	154 ± 4	157 ± 6	159 ± 6	165 ± 7	171 ± 9	156 ± 7	165 ± 4	167 ± 6	169 ± 5	177 ± 7	190 ± 10	168 ± 9

BCL: basic cycle length; SA: sinoatrial conduction interval; AH: atrio-His bundle conduction interval; HV: His-ventricular conduction interval; VRT: ventricular repolarization time interval; WCL: Wenckebach cycle length; AERP: atrial effective refractory period; AVNERP: AV nodal effective refractory period; HPFRP: His-Purkinje system functional refractory period; VERP: ventricular effective refractory period.

* $P<0.05$; ** $P<0.01$; *** $P<0.001$ compared to respective control value by ANOVA, followed by Dunnett's *t* test for multiple comparisons.

TABLE 2

Effects of HA-7 and d-sotalol on reperfusion-induced ventriclular fibrillation (VF)

Values of duration of VF are expressed as mean±s.e.m.

Treatment		*n*	Incidence of VF	Duration of VF (sec)
DMSO	0.06%	9	9/9 (100%)	397 ± 52
HA-7	30 μM	7	6/7 (86%)	124 ± 25
	100 μM	9	4/9 (44%)*	31 ± 15**†
d-Sotalol	30 μM	7	7/7 (100%)	216 ± 52
	100 μM	8	7/8 (88%)	129 ± 18**

* $P<0.05$ compared to vehicle control value by Fisher's exact test. ** $P<0.01$ compared to vehicle control value, while † $P<0.05$ compared to 100 μM d-sotalol group by ANOVA, followed by Dunnett's *t* test for multiple comparisons.

TABLE 3

Effects of HA-7 and d-sotalol on AERP and atrial fibrillation threshold (AFT) in the presence of adenosine

Values are expressed as mean±s.e.m.

Treatment		*n*	AERP (ms)	AFT (mA)
DMSO	Control	7	20 ± 2	1.5 ± 0.2
	0.06%	7	21 ± 1	1.7 ± 0.3
HA-7	Control	9	24 ± 2	1.5 ± 0.3
	30 μM	9	38 ± 3*	3.4 ± 1.3
	100 μM	9	62 ± 3***	13.6 ± 0.4***
d-Sotalol	Control	8	23 ± 2	1.5 ± 0.1
	30 μM	8	34 ± 3	1.8 ± 0.2
	100 μM	8	39 ± 4	3.9 ± 1.4

The AERP before adenosine treatment in DMSO, HA-7, and d-sotalol group are 49 ± 5, 57 ± 3, and 51 ± 4 ms, respectively, and AFT for all groups are larger than 14 mA.

* $P<0.05$ and *** $P<0.001$ compared to respective control value by ANOVA, followed by Dunnett's *t* test for multiple comparisons.

JPET Fast Forward. Published on September 20, 2005 as DOI: 10.1124/jpet.105.092106
This article has not been copyedited and formatted. The final version may differ from this version.

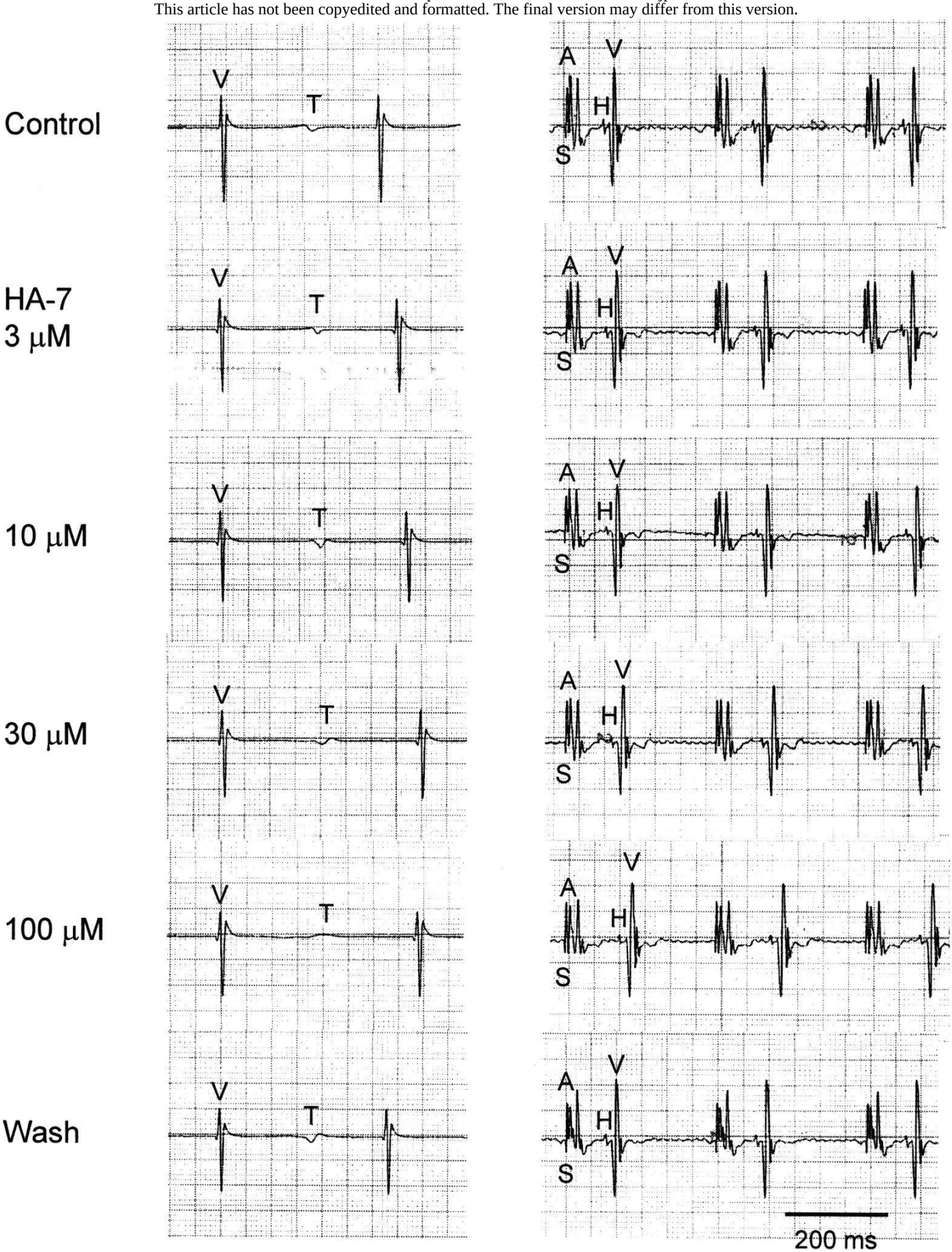

Figure 1

JPET Fast Forward. Published on September 20, 2005 as DOI: 10.1124/jpet.105.092106
This article has not been copyedited and formatted. The final version may differ from this version.

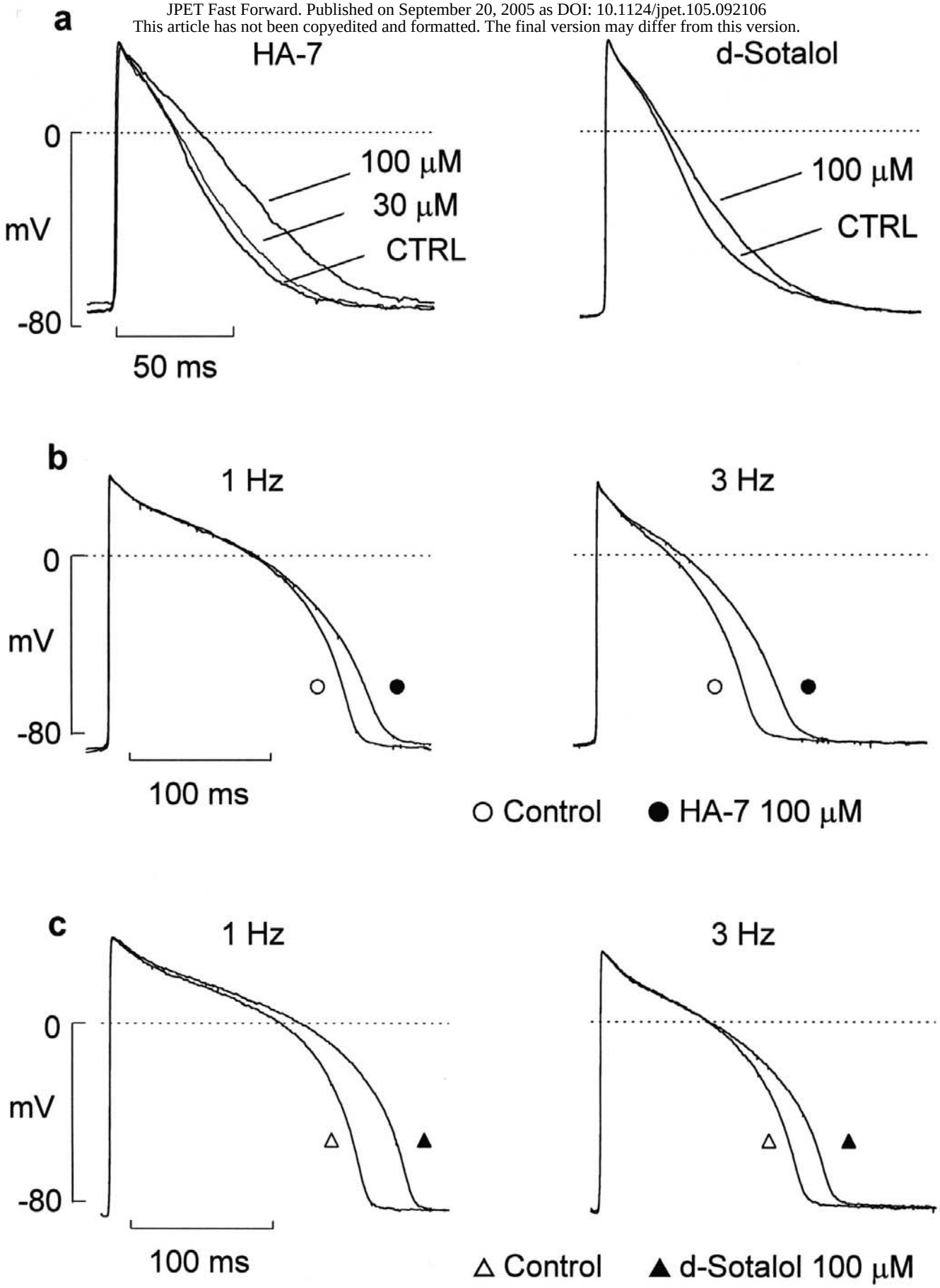

Figure 2

JPET Fast Forward. Published on September 20, 2005 as DOI: 10.1124/jpet.105.092106
This article has not been copyedited and formatted. The final version may differ from this version.

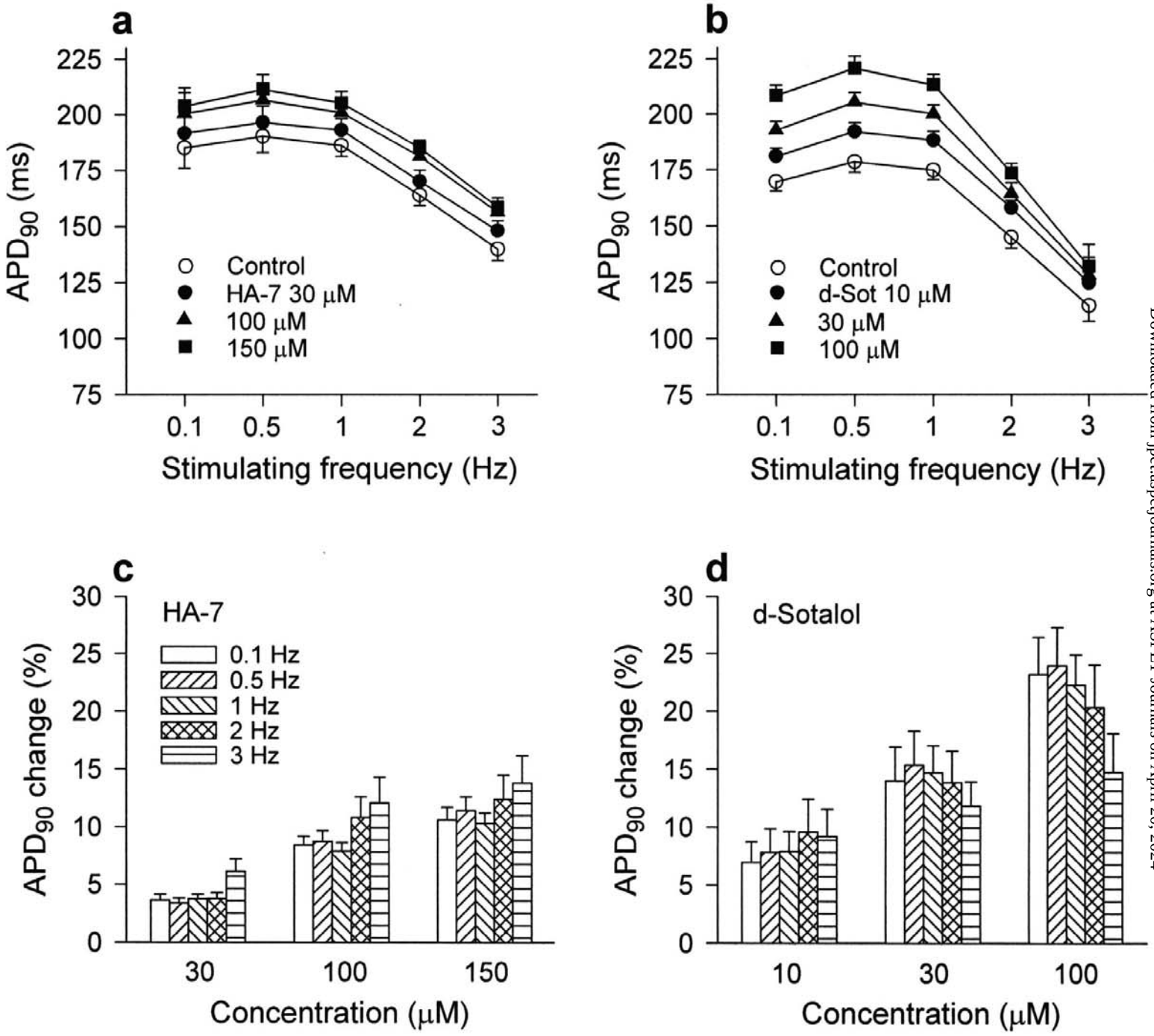

Figure 3

JPET Fast Forward. Published on September 20, 2005 as DOI: 10.1124/jpet.105.092106
This article has not been copyedited and formatted. The final version may differ from this version.

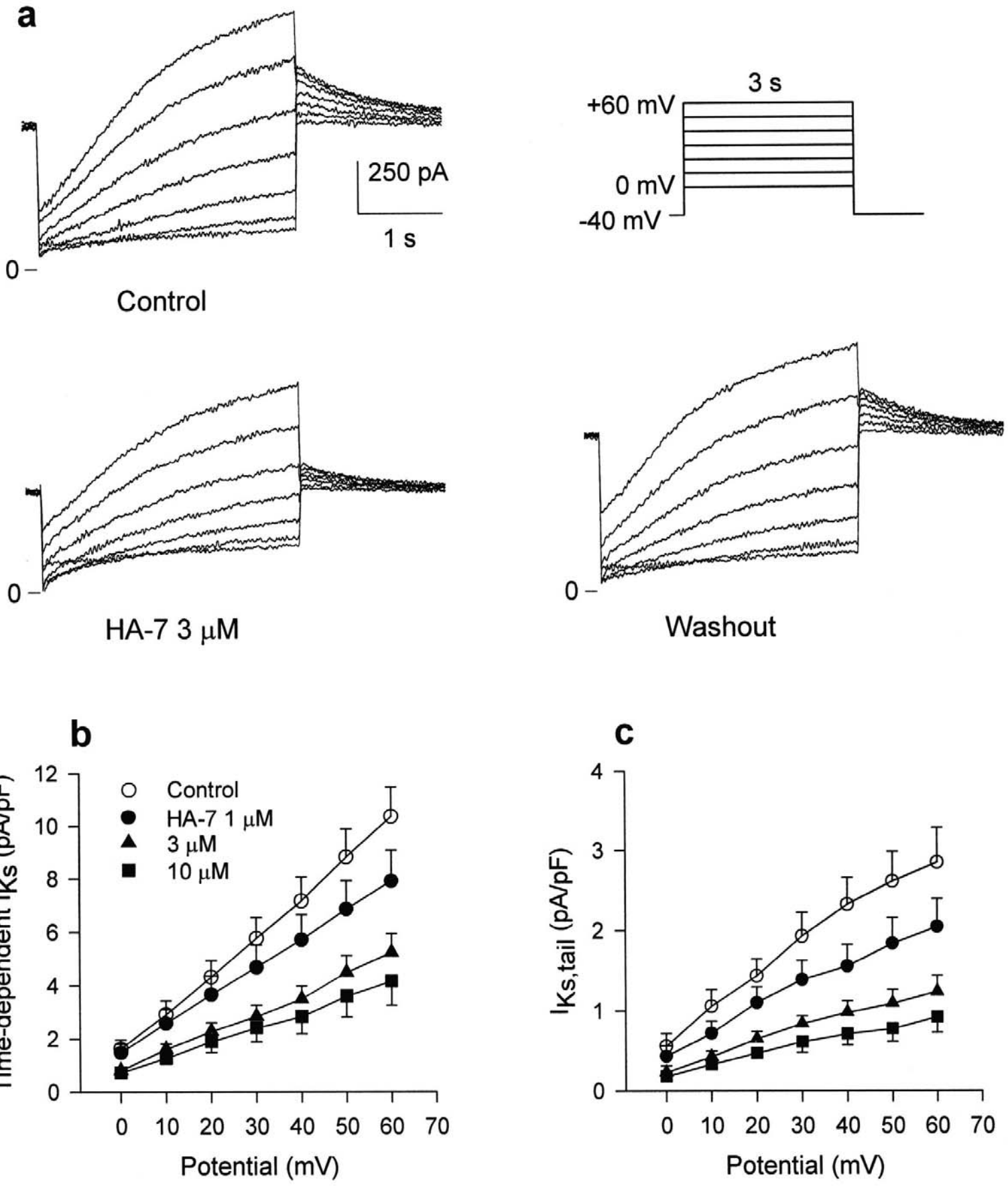

Figure 4

JPET Fast Forward. Published on September 20, 2005 as DOI: 10.1124/jpet.105.092106
This article has not been copyedited and formatted. The final version may differ from this version.

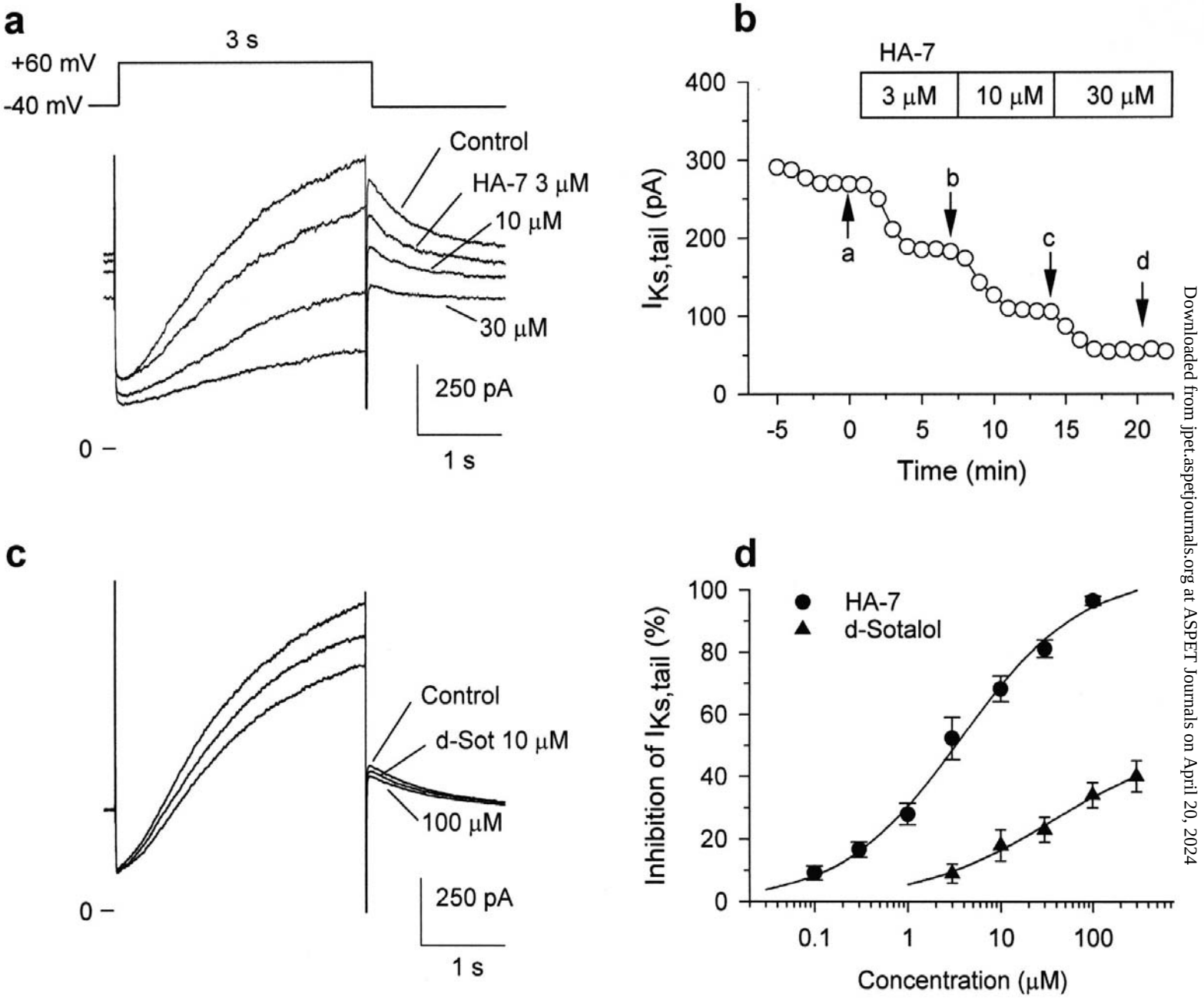

Figure 5

JPET Fast Forward. Published on September 20, 2005 as DOI: 10.1124/jpet.105.092106
This article has not been copyedited and formatted. The final version may differ from this version.

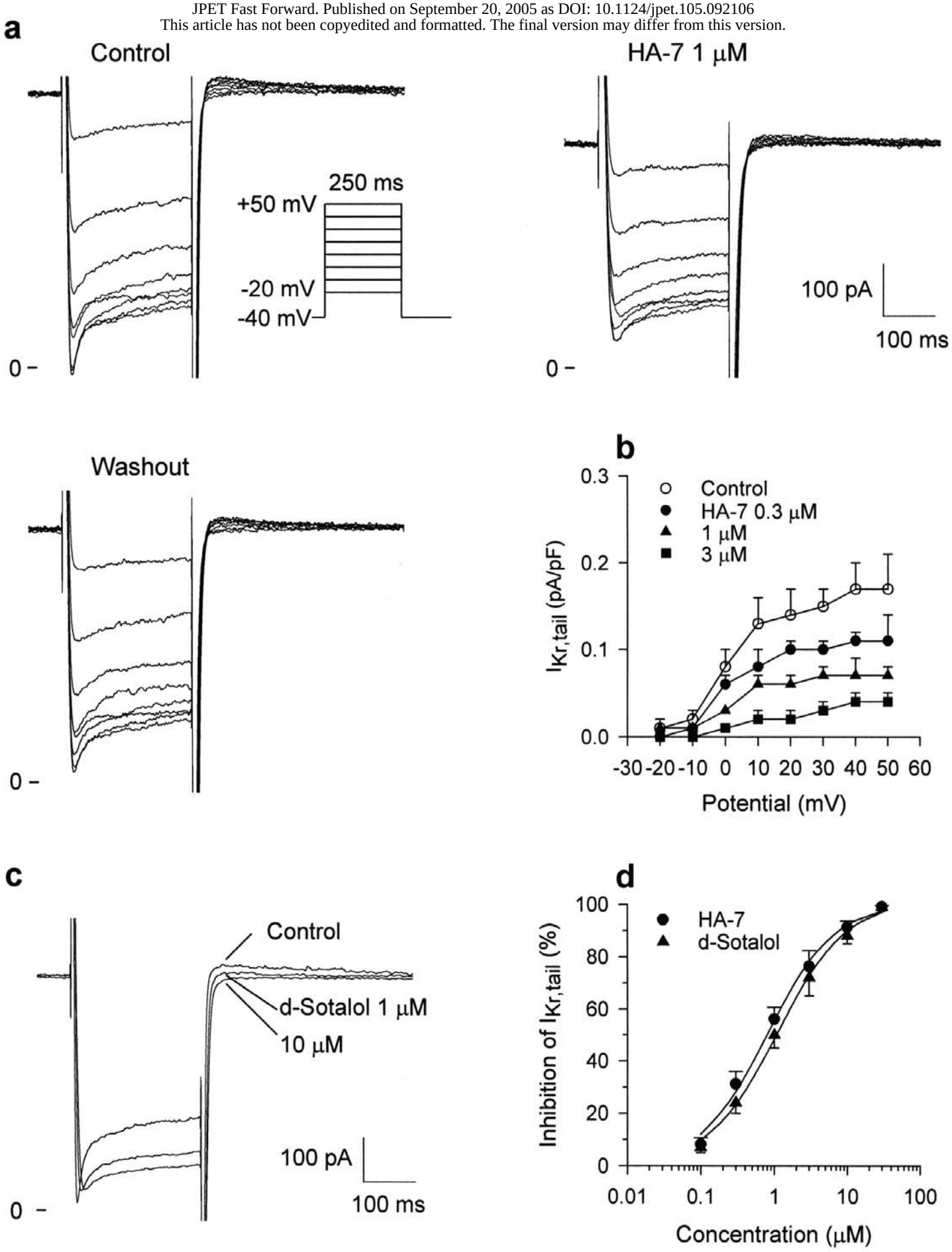

Figure 6

JPET Fast Forward. Published on September 20, 2005 as DOI: 10.1124/jpet.105.092106
This article has not been copyedited and formatted. The final version may differ from this version.

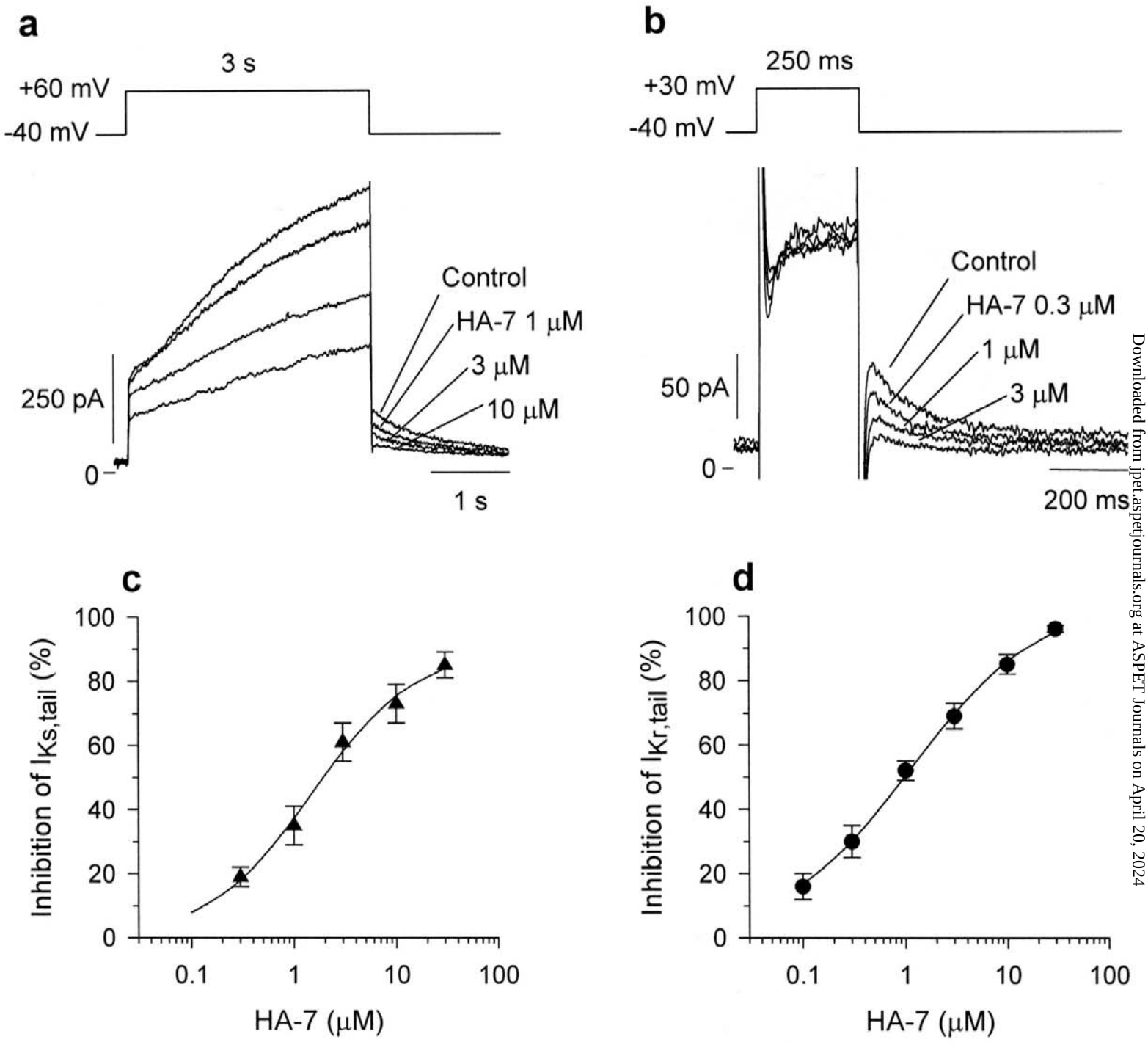

Figure 7

JPET Fast Forward. Published on September 20, 2005 as DOI: 10.1124/jpet.105.092106
This article has not been copyedited and formatted. The final version may differ from this version.

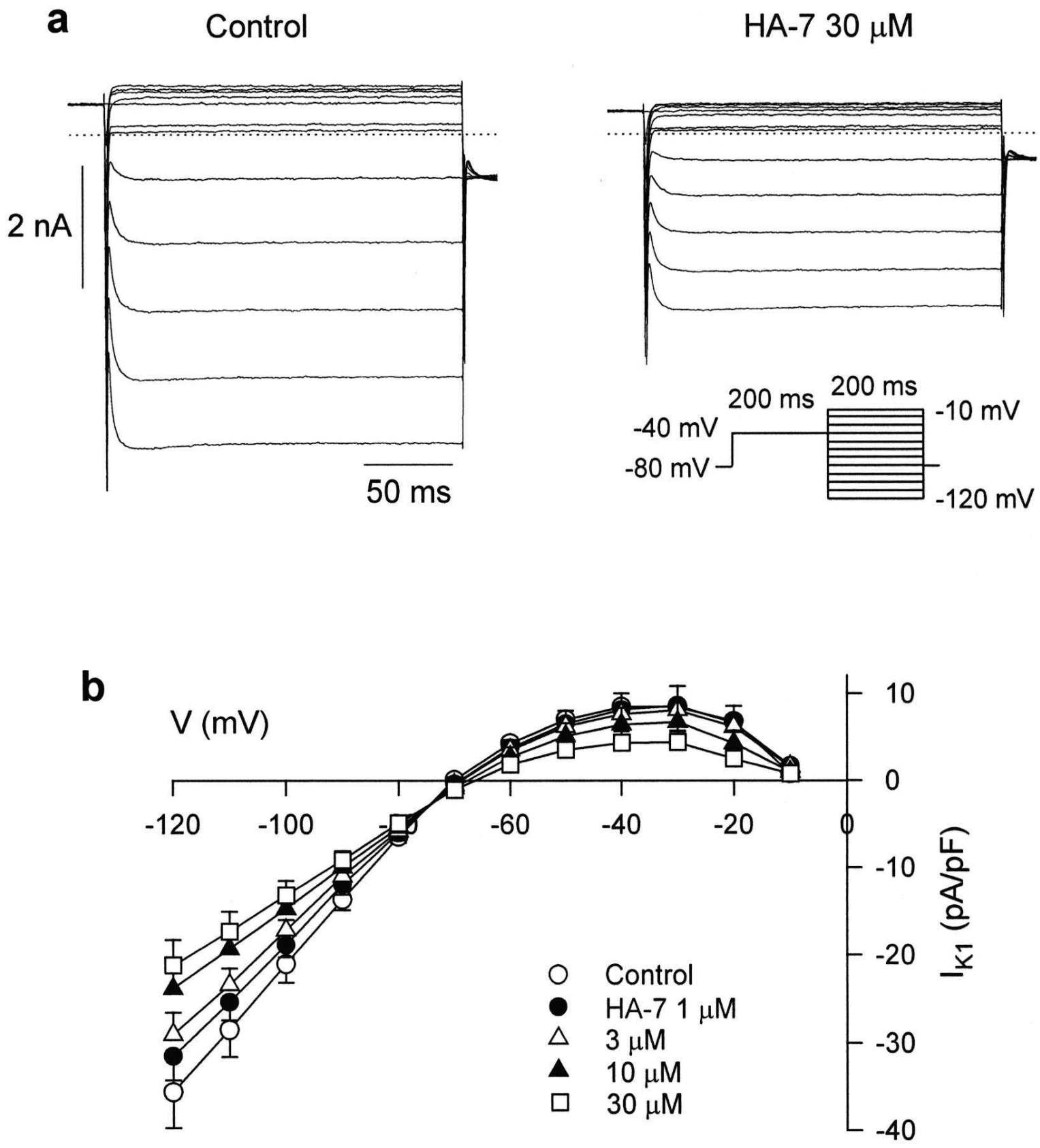

Figure 8

JPET Fast Forward. Published on September 20, 2005 as DOI: 10.1124/jpet.105.092106
This article has not been copyedited and formatted. The final version may differ from this version.

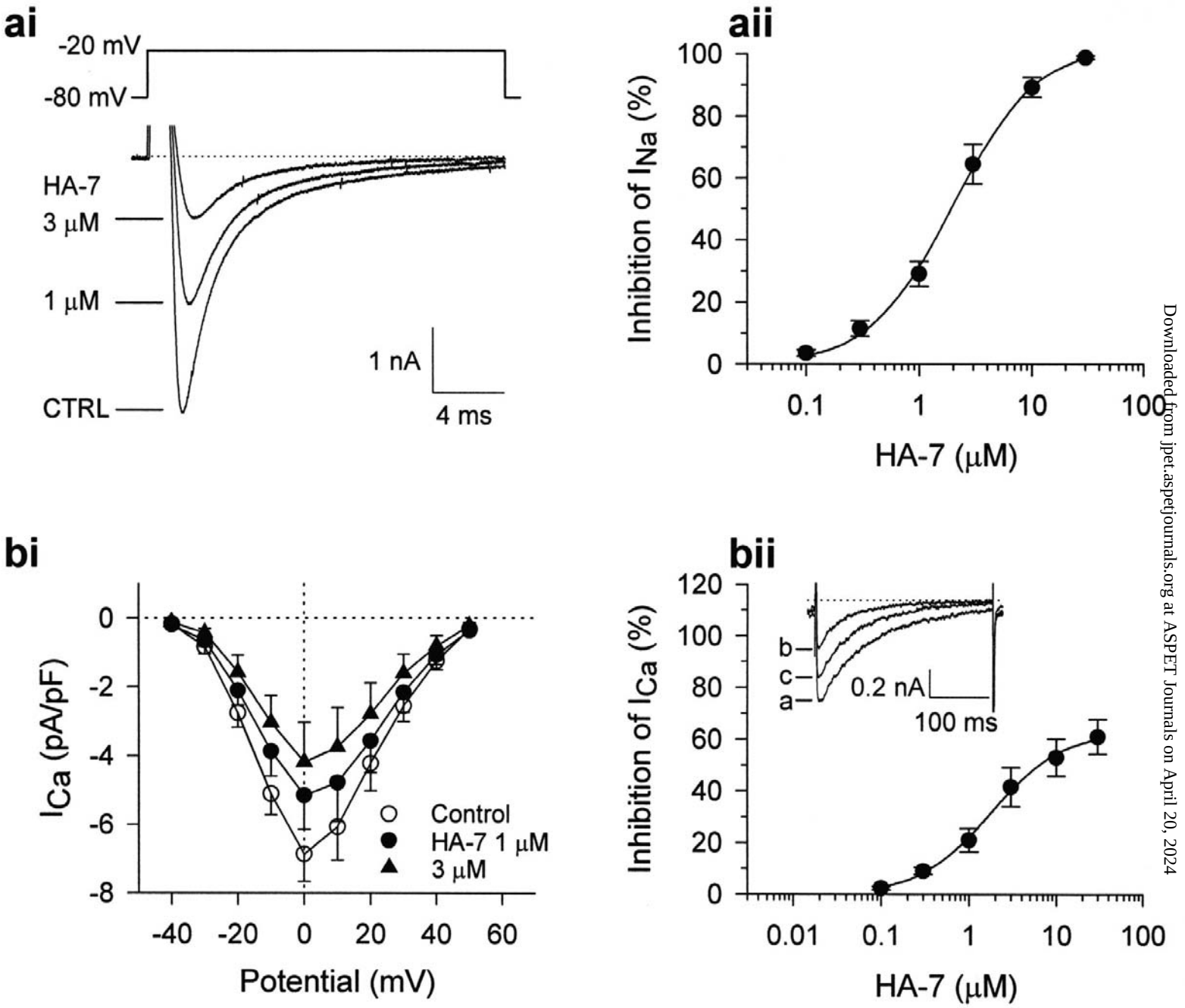

Figure 9